International Journal of Hydrological and Environmental for Sustainability
Volume 1, Issue 3, 120-131
e_ISSN: 2828-5050
https://www.journal.foundae.com/index.php/ijhes

Preparation and Application of Magnetite (Fe_3O_4) Nanoparticles by Co-precipitation Method for Removal Rhodamine B in Wastewater

Ganesha Antarnusa*
Department of Physics Education,
Universitas Sultan Ageng Tirtayasa,
INDONESIA

***Correspondence: E-mail:** ganesha.antarnusa@untirta.ac.id

Article Info

Article history:

Received: October 02, 2022
Revised: October 25, 2022
Accepted: October 28, 2022

Abstract

Fe_3O_4 coated with PEG has been successfully synthesized using co-precipitation method to reduce RhB. From the XRD results, it can be seen that all samples are Fe_3O_4 with the highest Miller index at (311). The crystallinity of Fe_3O_4 was maintained even though PEG was added. From the SEM-TEM analysis, it can be seen that the two samples have a uniform size distribution. Then, PEG can increase the dispersibility of the sample. From the FTIR analysis it was confirmed that there was PEG content in Fe_3O_4. From the results of the VSM analysis, it was confirmed that the sample has nearly superparamagnetic properties with a small *Hc* value. Then, Fe_3O_4 and Fe_3O_4/PEG were used to remove RhB in water by magnetic separation process. From the results of the study, it was obtained that the optimum absorption occurred in several parameters, namely the initial concentration of RhB at 100 mg/mL, with a pH of 6, the dose of Fe_3O_4/PEG at 0.8 g/L and a contact time of 40 minutes at room temperature. At this optimum condition, the absorption has a color removal of 31.1%.

Keywords: Fe_3O_4; Co-precipitation; magnetism; rhodamine B; wastewater

To cite this article: Antarnusa, G. (2022). Preparation and application of magnetite (Fe_3O_4) nanoparticles by co-precipitation method for removal Rhodamine B in Wastewater. *International Journal of Hydrological and Environmental for Sustainability, 1*(3), 120-131. https://doi.org/10.58524/ijhes.v1i3.140

INTRODUCTION

Over the last few decades there has been an increase in industrial activity. As a result, wastewater from various industries like battery manufacturing industries, mining, chemical manufacturing, tannery, etc., contain toxic heavy metals that cannot be decomposed and have a tendency to accumulate in living organisms which can cause numerous diseases and health problems (Shen, 2009). The waste released from the dye industry is a major environmental problem because it interferes with aesthetics. In addition, some dyes are also toxic or carcinogenic. The presence of colored waste not only interferes with aesthetics, but also inhibits light penetration thereby regulating biological processes in rivers. It is estimated that 10-50% of the dye is lost in the dyeing process waste (Anirudhan, 2009). Therefore, the treatment of liquid waste containing dyes is a concern because it can harm the receiving waters (Zhu, 2011). For example, Rhodamine B (RhB) is one of the most frequently used dyes and is present in wastewater from several different industries (Peng, 2012). The heavy metal content and chemical properties of RhB are harmful to human health (WHO, 2000). One of the dangerous aspects of RhB is that it has a radical alkylation compound (CH_3-CH_3). Consequently, it can bind to DNA, fats and proteins (Kurniawan, 2018). In addition, RhB also contains chlorine compounds (Cl). Chlorine compounds are dangerous and reactive halogen compounds that are toxic to the body. If ingested, this compound will try to achieve stability by

binding to other compounds. The use of this dye has been banned in Europe since 1984 because Rhodamine B is a strong carcinogen (cancer causing). The Rhodamine B toxicity test conducted on mice and rats has proven its carcinogenic effect. Consumption of RhB in the long term can cause accumulation and can cause physiological disturbances, liver damage, impaired liver function, symptoms of enlarged liver and kidneys or can even cause liver cancer. Thus, it is urgent to clean RhB from effluents to achieve industrial effluent standards before being discharged into the environment (Veisi, 2019). At the same time, in recent years the textile market has grown significantly. In other words, there is the potential to increase the content of Rhodamine B in the water. Therefore, purifying water before use is very important because clean water is one of the basic needs for human existence. Moreover, in recent decades the massive dumping of heavy metals has caused worldwide concern.

Numerous techniques and treatment processes have been used to for the removal of heavy metals from wastewater, including membrane separation, reverse osmosis, solvent extraction, evaporation, precipitation, ion exchange and so on. However, for the application of disposal and treatment of residual metal deposits, some of these methods have several disadvantages, namely high operational and capital costs (Benalia, 2021; Sultan, 2019; Akyol, 2020). Hence, much effort is being made to develop technologies for removing contaminants from aqueous solutions with low-cost materials. Fortunately, recent developments in nano-techniques have shed light on this field. Fe_3O_4 nanoparticles hold tremendous assure in the field of magnetic sensing, magnetic recording, environment, catalysts, magnetic drug targets, medical treatment, magnetic resonance imaging and recording materials for clinical diagnosis in recent decades (Yongsheng, 2022; Ruiz, 2019; Zhang, 2018). Several studies have revealed that magnetic nanoparticles produce a higher adsorption capacity to remove metals due to the limited size effect or high surface-to-volume ratio. Furthermore, by using an external magnetic field, an easy separation of the metal-charged magnetic absorber from the solution can be achieved.

Several methods to obtain Fe_3O_4 can be used, for example co-precipitation (Jesus, 2020), tridax procumbens leaf extract (Ramesh, 2018), ultrasonic-assisted impregnation (Dobaradaran, 2018), reducing agents (Qian, 2019), energy milling (Dewi, 2018), etc. The preparation method is very important to determine the characteristics of Fe_3O_4 such as morphology and size distribution. The most widely used method to prepare Fe_3O_4 is co-precipitation because the process is simple and low cost. In addition, chemical co-precipitation can produce fine stoichiometric particles of single and multicomponent metal oxides (Antarnusa, 2021). Several recent studies have shown that magnetic Fe_3O_4 can be used for wastewater purification, such as to adsorb Cadmium (II), Nickel (II), zinc (II), Copper (II), Mercury (II), Chromium (III, VI), Lead (II) and multiple metals matrix (Jabbar, 2022; Rangabhashiyam, 2022). Fe_3O_4 can also be used to remove natural organic compounds, pulp mill effluent color, hardness, desalination and alkalinity (Moosavi, 2020). After adsorption, Fe_3O_4 can be separated from the medium by a simple magnetic process. Thus, the economical, scalable, non-toxic and efficient synthesis of Fe_3O_4 nanoparticles is of great interest for potential applications and fundamental research (Eskandari, 2021; Song, 2018). However, pure Fe_3O_4 is easily oxidized and easily agglomerates in water (Demirezen, 2022). PEG is usually used as a coating on Fe_3O_4 as a protective reagent and dispersing agent (Chavan, 2019). In previous studies, Fe_3O_4 has been coated by several organic substances like diethylene triamine pentaacetic acid (DTPA) and oleic acid (OA) as a stable material for Fe_3O_4 and its functional groups have an adsorption effect on heavy metals (Salman, 2021).

In this study, we carried out research on the purification of artificial wastewater containing RhB, using magnetite Fe_3O_4 nanoparticles and PEG-coated Fe_3O_4 nanoparticles. Many techniques for removing dyes from sewage have been developed, including adsorption, photocatalytic oxidation, sonochemical treatment and electrochemical treatment. Of these several methods, the adsorption method is a promising and attractive alternative for the treatment of wastewater containing RhB if the adsorbent used is cheap and available (Bilgic, 2022; Ojemaye, 2019; Zhang, 2020). We found that Fe_3O_4/PEG can effectively absorb toxic metal ions in wastewater. Furthermore, the adsorption efficiency was confirmed by conducting a series of experiments with several variations of concentration of RhB, pH, dosage of Fe_3O_4/PEG and contact time. It is hoped that this investigation will contribute to the current water purification industry.

METHOD

Chemical

All chemicals were of analytical grade and used as received without any further purification. Ferrous chloride tetrahydrate ($FeCl_2.4H_2O$, 99%), ferric chloride hexahydrate ($FeCl_3.6H_2O$, 99%), polyethylene glycol-4000 (PEG-4000) and Ammonium hydroxide (NH_4OH, 25 %) were purchased from Merck-Germany. All aqueous solutions were prepared with distilled water.

Preparation of PEG-Fe_3O_4

PEG-coated Fe_3O_4 were synthesized by co-precipitation method. First, 0.25 g of $FeCl_2 \cdot 4H_2O$ and 0.68 g of $FeCl_3 \cdot 6H_2O$ (with a molar ratio of Fe^{2+}:Fe^{3+} = 1:2) were dissolved in 25 ml of distilled water while stirring to obtain a solution of ferrous ions. Then, 25 ml of NH_4OH (25%) was slowly dripped into this solution with stirring at 500 rpm. Next, the suspension was stirred at 40°C for 30 minutes and uncoated Fe_3O_4 (nanoparticle core) was obtained. Then, the precipitation process is carried out using a permanent magnetic field placed under the solution. Then the precipitate was washed seven times and the supernatant was poured. Furthermore, for the purpose of coating, Fe_3O_4 which is still wet was dissolved in distilled water. Then the PEG was dissolved in distilled water and added to the Fe_3O_4 solution. Then the mixed solution was stirred for 60 minutes at a speed of 500 rpm. After the reaction, the coated Fe_3O_4 was deposited by a magnet and washed several times to remove excess polymer. Then the samples were dried in an oven at 50°C for 12 hours (Karagaac, 2022).

Characterization

The XRD diffraction patterns were carried out using XRD; PANalytical X'Pert PRO diffractometer to determine the crystal structure of the smples in the range 10°-90° using a Cu-Kα radiation (λ=0.15406 nm) at 40 kV and 15 mA. Fourier transform infrared (FTIR) spectra of all the samples were collected on Parkin Elmer Frontier Optica spectrometer using KBr pellet technique in the 4000-400 cm−1 range. The mean particles, size distribution and morphology of samples was observed by scanning electron microscopy (SEM; JEOL JIB 4610F) and transmission electron microscope (TEM; JEOL-JEM-1400). Magnetic measurements were studied with vibrating sample magnetometer (VSM; Dexing VSM250) measurement system with magnetization loops up to 10 kOe fields at room temperature.

Adsorbtion

The adsorption of RhB by Fe_3O_4 and Fe_3O_4/PEG was carried out at a temperature of 25°C by the adsorption method. The RhB solution was prepared by dissolving an appropriate amount of RhB in distiled water to give a final concentration range from 25 to 150 mg/mL. The pH of the suspension mixture was adjusted between 5-9 using hydrogen chloride (HCl) and sodium hydroxide (NaOH). In general, doses of Fe_3O_4/PEG were 0.5, 0.6, 0.7, 0.8, 0.9 and 1 g was added to 1 L of RhB solution, and the resulting suspension mixture was carried out at about 500 rpm at room temperature in a shaking incubator. In addition, contact times at 15, 30, 45, 60 and 75 minutes were also performed. The solid magnetite nanoparticles are then separated from the suspension using permanent magnets. UV-Vis was used to determine the amount of RhB remaining in solution. The removal rates η,(%) and adsorption capacity (q_e) were calculated according to the following equation 1 and 2:

$$\eta\ (\%) = \frac{(C_o - C_e) \times 100}{C_o} \quad (1)$$

$$q_e = \frac{(C_o - C_e)V}{m} \quad (2)$$

Where, C_o is the initial absorbance, C_e is the equilibrium absorbance in the solution (mg/mL), m is the mass of the Fe_3O_4 and Fe_3O_4/PEG (g), V is the volume of RhB solution (L) and q_e is the equilibrium adsorption capacity per gram of the Fe_3O_4 and Fe_3O_4/PEG (g/L) (Bilgic, 2022).

RESULTS AND DISCUSSION

X-ray diffraction (XRD)

Figure 1 shows the XRD patterns of Fe_3O_4 and Fe_3O_4/PEG, respectively. In pattern of Fe_3O_4 the distinct peaks correspond to crystal planes 220, 311, 400, 422, 511, and 440 of a cubic spinel structure of Fe_3O_4. Furthermore, from patterns of Fe_3O_4/PEG the observed diffraction patterns of Fe_3O_4/PEG nanoparticles showed that the crystal structure of Fe_3O_4 was maintained, even after being coated with PEG (Guo, 2015).

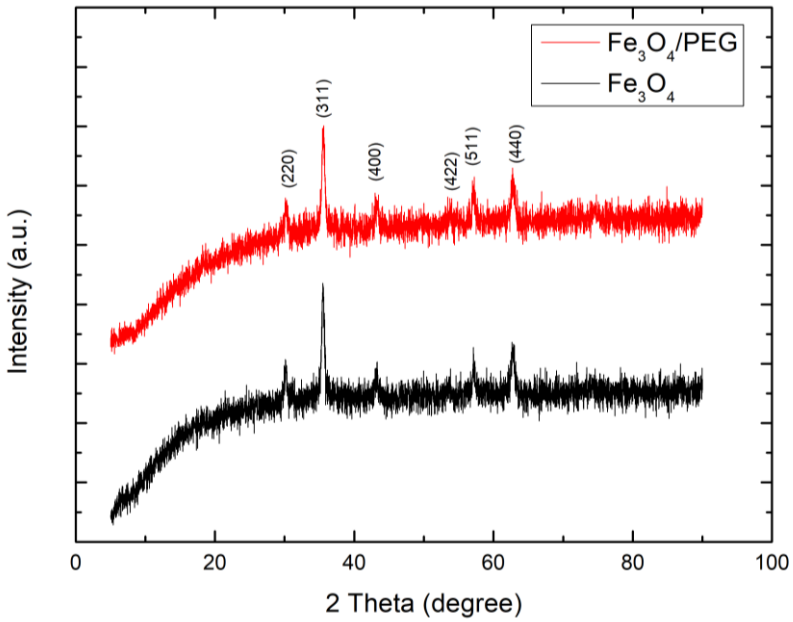

Figure 1. XRD patterns of Fe_3O_4 and Fe_3O_4/PEG

Fourier-transform infrared spectroscopy (FTIR)

Figure 2 presents the FTIR spectra of the Fe_3O_4 and Fe_3O_4/PEG. The signature band of Fe−O stretching mode in Fe_3O_4 was observed at 567 cm^{-1} (Sobeh, 2022). The peak obtained at 1134 cm^{-1} is attributed to the vibrations of the C−O−C bonds (Da, 2022). The band observed at 1630 is due to C=O stretching vibration band of PEG (Antarnusa, 2020). The peak at 2931 cm^{-1} indicates stretching vibration of C−H. For two shapes of samples, the broad peaks at about 3423 and 3170 cm^{-1} are attributed to the O−H vibrations (Namikuchi, 2021). Thus, the data confirmed the formation of PEG in the Fe_3O_4.

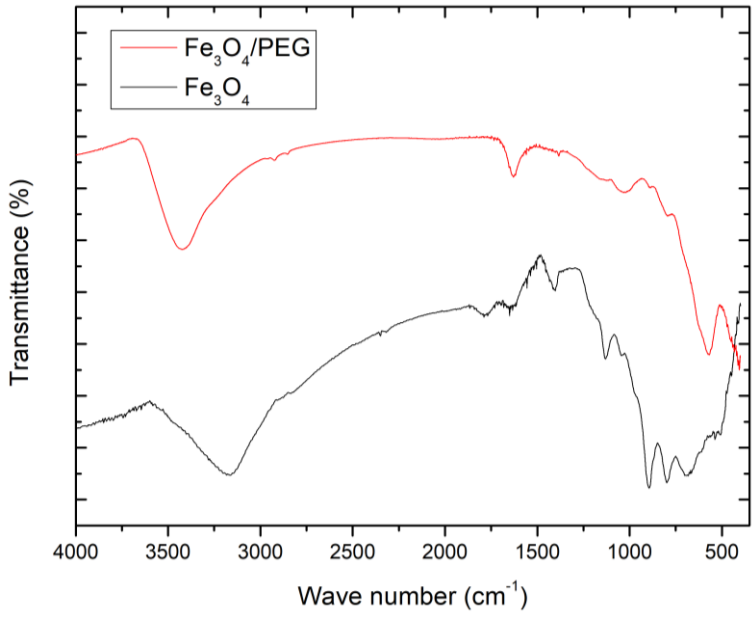

Figure 2. FTIR spectra of Fe_3O_4 and Fe_3O_4/PEG

Scanning Electron Microscope (SEM) and transmission electron microscope (TEM)

The SEM analysis was applied to investigate the surface morphology of the synthesized materials as shown in **Figure 3**. The Fe_3O_4 have a nearly spherical shape, and the average size of Fe_3O_4 was estimated to be about 32 nm (Da, 2022). The SEM images of the Fe_3O_4/PEG showed that the prepared nanoparticles possess a nearly spherical shape in relatively uniform distribution with an average diameter of about 22 nm, which can be attributed to the addition of PEG acting as a stabilizer and dispersing agent (**Figure 3b**) (Karimi, 2021). **Figure 4** shows the morphology of Fe_3O_4 and Fe_3O_4/PEG were analyzed by transmission electron microscope. The particle size distribution of Fe_3O_4 and Fe_3O_4/PEG NPs are 12 and 11 nm, respectively (Janani, 2021).

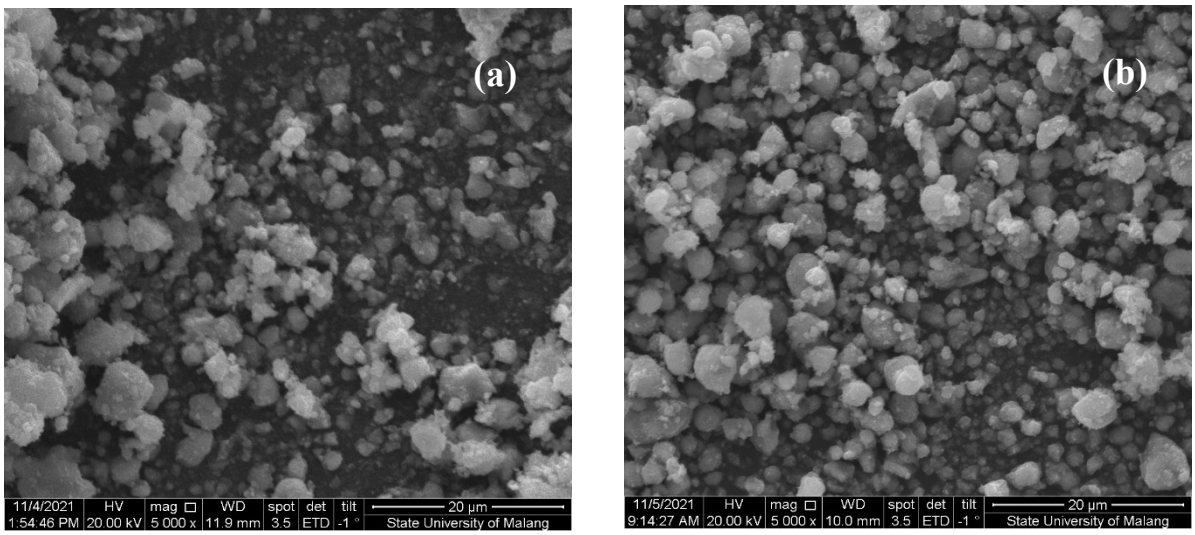

Figure 3. SEM images of (a) Fe_3O_4 and (b) Fe_3O_4/PEG

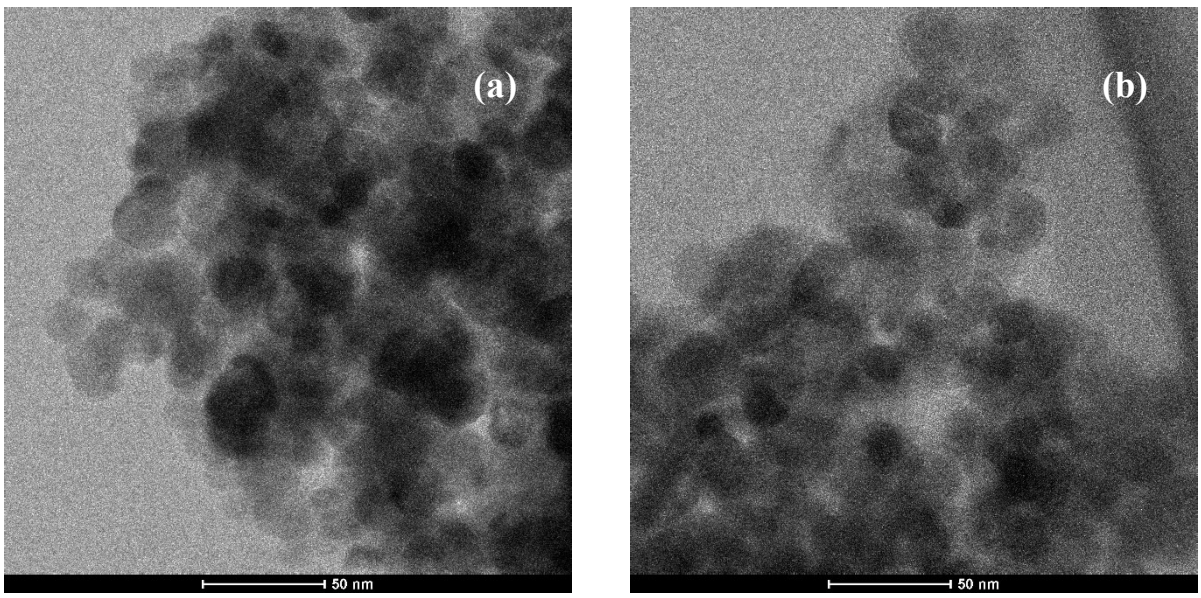

Figure 4. TEM images of (a) Fe_3O_4 and (b) Fe_3O_4/PEG

Vibrating-sample magnetometer (VSM)

Figure 5 presents the magnetization loops of the samples. All samples exhibit a soft ferromagnetic behavior with small remanence and coercivity value. The saturation magnetization of the samples are 59.16 and 55.34 emu/g corresponding to the Fe_3O_4 and Fe_3O_4/PEG, respectively. Compared with the research conducted by (Frei, 1957) demonstrated the possibility that ferromagnetic materials exhibit behavior that tends to be nearly superparamagnetic before reaching a measure of single-domain behavior. This can be attributed to the material being above the blocking

temperature and pin energies of the regular motion of the domain walls. Several studies have concluded that saturation magnetization increases and coercivity decreases with decreasing surface anisotropy (Seal, 2021). In present study, the coercivity values were maintained from the Fe_3O_4 indicating that the surface anisotropy of Fe_3O_4/PEG was increased. Since the shape and size of Fe_3O_4/PEG is not much different from that of Fe_3O_4, it can be assumed that the surface modification in the sample plays an important role. The presence of PEG as a non-magnetic material in the sample causes a decrease in its M_S value, as is also seen in Fe_3O_4/PEG. The influx of cations towards the octahedral sites is increased for the Fe_3O_4/PEG compared to Fe_3O_4, which is known to increase the resulting magnetic moment of spinel Fe_3O_4. Hence, it can be determined that the properties of the PEG group through which Fe_3O_4 acts as an dispersing agent affect the separation of the Fe ion crystal field, as illustrated in XRD (Suharyadi, 2021).

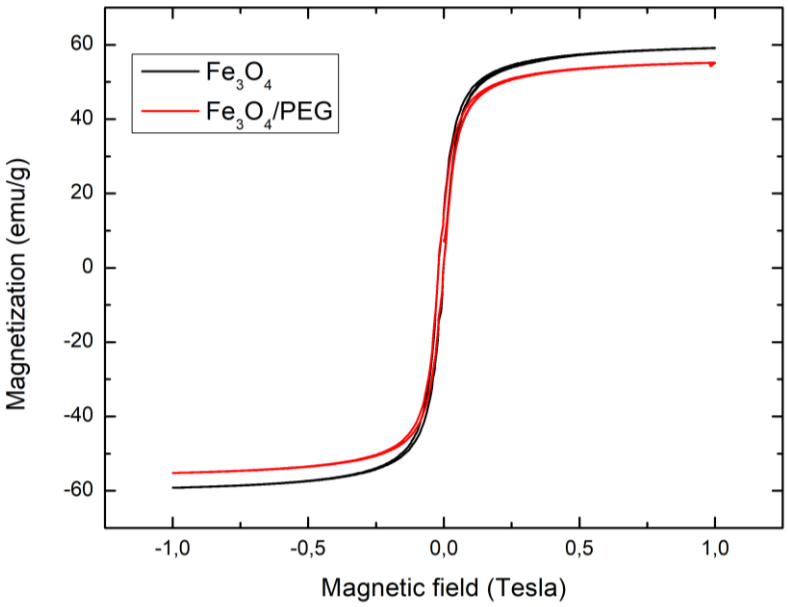

Figure 5. Magnetization curves of Fe_3O_4 and Fe_3O_4/PEG

Adsorbtion activity

To determine the effect of RhB concentration on RhB degradation, 25, 50, 75, 100, 125 and 150 mg/L RhB solutions were used as shown in **Figure 6**. The degradation effect inreased from 22.8% to 33.5%, when the concentration RhB increased from 25 mg/L to 150 mg/L. It can be seen that the dcolor removal at the initial RhB concentration affects a large number of vacant sites available for adsorption during the initial stage. The initial concentration of RhB in the adsorption process was then used at a concentration of 100 mg/mL (Zhang, 2017).

One of the fundamental parameters that affect the removal of organic pollutants is the pH value of the solution. Hence, the effect of pH on the degradation of RhB in the system was explored by adjusting the pH of the solution to 5, 6, 7, 8 and 9. As shown in **Figure 7**, the highest RhB degradation rate was observed at pH 5. On the other hand, low degradation rates were observed under neutral and alkaline conditions. Below the optimal pH, the absorption mainly results from electrostatic attraction (Leng, 2013). The color removal of RhB at pH 6 is 25.1%, not much different from pH 5. Thus, the adsorption process is used at pH 6 because it is close to the pH of a neutral solution.

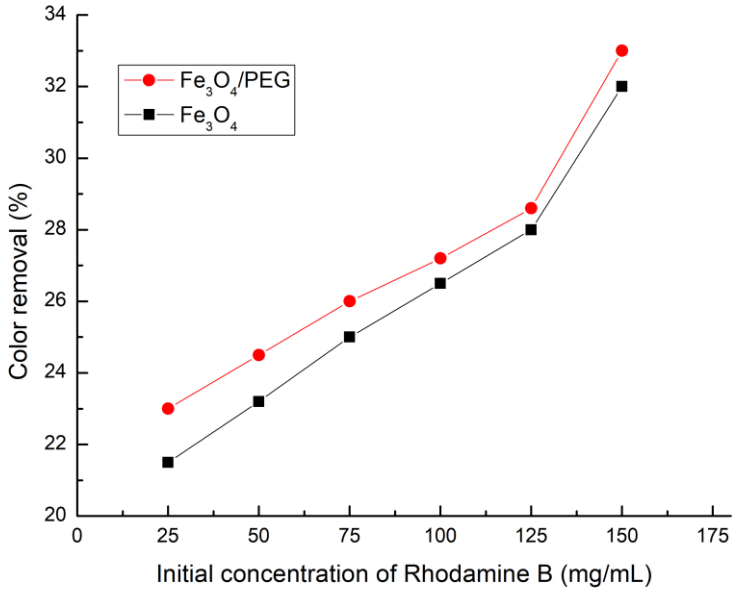

Figure 6. Effect of initial concentration of rhodamine B

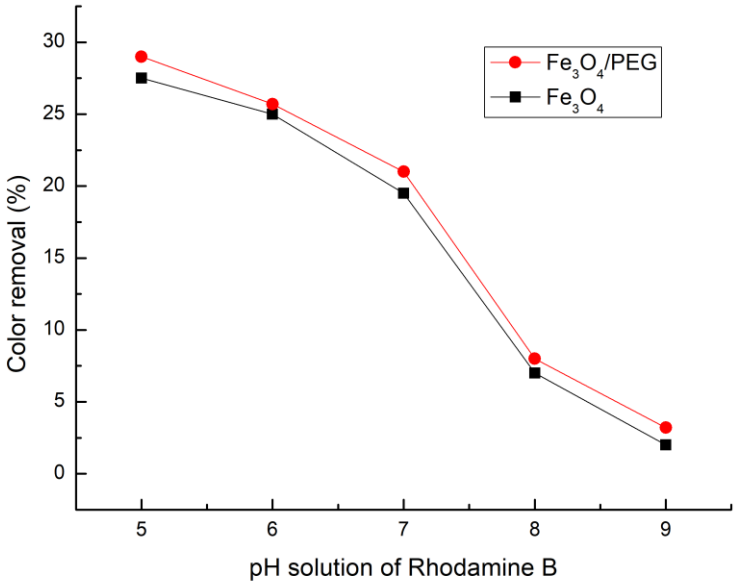

Figure 7. Effect of pH solution of Rhodamine B

As one of the important applications, the synthesized Fe_3O_4/PEG nanoparticles are used to treat wastewater containing RhB (Wang, 2013). In this study, to treat wastewater containing RhB, synthesized Fe_3O_4 and Fe_3O_4/PEG with different doses were used. Chemical analysis of several sorbents in wastewater before and after treatment showed clearly that the adsorption capacity using different concentrations resulted in different removal percentages (Iorio, 2019). As shown in **Figure 8**, it is clear that the adsorption capacity of Fe_3O_4/PEG particles increases with decreasing surface area. Thus it can be concluded that the effect of particle size (or surface-to-volume ratio) on the removal of RhB from solution is dramatic (Shen, 2009).

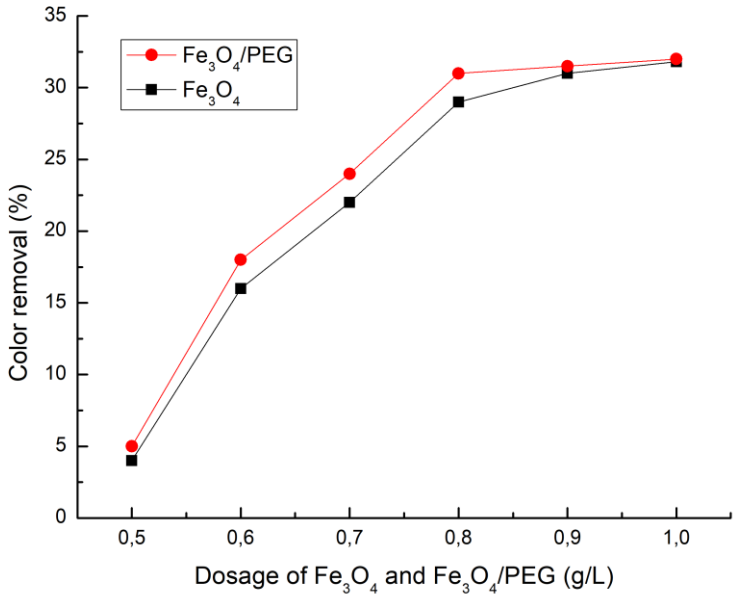

Figure 8. Effect of dosage of Fe_3O_4 and Fe_3O_4/PEG.

The effect of contact time on decolorization was also observed. It is seen that decolorization increases with increasing contact time as shown in **Figure 9**. After 40 min saturation occurs and after equilibrium time decolorization stabilizes (Ai, 2011). At the optimum condition the adsorption has a color removal of 31.1%. This decolorization condition is optimal so that the extra time does not add to the decolorization (Jiao, 2018).

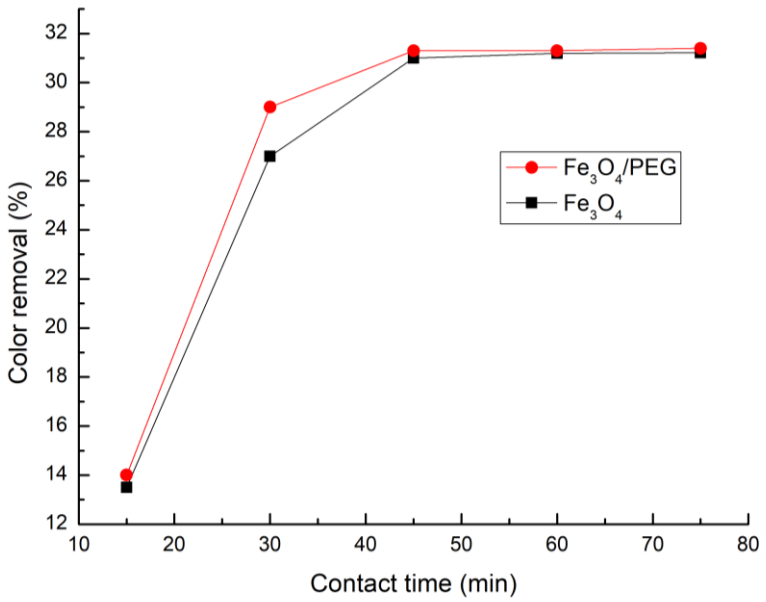

Figure 9. Effect of contact time adsorption of Rhodamine B

CONCLUSION

In this study, Fe_3O_4/PEG was synthesized using co-precipitation method. The properties of the samples were confirmed using XRD, FTIR, SEM, TEM and VSM. Fe_3O_4 and Fe_3O_4/PEG were found to have a homogenous particle size distribution. The addition of PEG can increase the homogeneity of distribution. In addition, the saturation magnetization decreased with the addition of PEG. Then,

Fe_3O_4 and Fe_3O_4/PEG were used as RhB degraders. The addition of PEG can increase the removal effect because the surface distribution effect is increasing. By using several parameters, such as the initial concentration of RhB at 100 mg/mL, with a pH of 6, the dose of Fe_3O_4/PEG at 0.8 g/L and a contact time of 40 minutes at room temperature, the optimum absorbance was obtained. At this optimum condition, the absorption has a color removal of 31.1%.

ACKNOWLEDGMENT

The authors would like to thank all reviewers who have provided suggestions to improve this article.

CONFLICTS OF INTEREST

The authors declare no conflict of interest concerning the publication of this article. The authors also confirm that the data and the article are free of plagiarism.

REFERENCES

Ai, L., Zeng, C., & Wang, Q. (2011). One-step solvothermal synthesis of Ag-Fe_3O_4 composite as a magnetically recyclable catalyst for reduction of Rhodamine B. Catalysis Communications. 14, 68–73. https://doi:10.1016/j.catcom.2011.07.014.

Anirudhan, T. S., Jalajamony, S., & Divya, L. (2009). Efficiency of Amine-Modified Poly(glycidyl methacrylate)-Grafted Cellulose in the Removal and Recovery of Vanadium(V) from Aqueous Solutions. Industrial & Engineering Chemistry Research. 48, 2118–2124. https://doi.org/10.1021/ie8000869.

Antarnusa, G., Denny, Y.R., Suherman, A., Utami, I.S., & Saefullah, A. (2021). The Effect of Additional Polyethylene Glycol (PEG) as Coating Fe_3O_4 for Magnetic Nanofluid Applications. Recent Innovations in Chemical Engineering. 14, 335-346. https://doi.org/10.2174/2405520414666210325122511.

Antarnusa, G., & Suharyadi, E. (2020). A synthesis of polyethylene glycol (PEG)-coated magnetite Fe_3O_4 nanoparticles and their characteristics for enhancement of biosensor. Materials Research Express. 7, 056103. https://doi.org/10.1088/2053-1591/ab8bef.

Akyol, Ç., Foglia, A., Ozbayram, E.G., Frison, N., Katsou, E., Eusebi, A.L., & Fatone, F. (2020). Validated innovative approaches for energyefficient resource recovery and re-use from municipal wastewater: From anaerobic treatment systems to a biorefinery concept. Critical Reviews in Environmental Science and Technology. 50(9), 869-902. https://doi.org/10.1080/10643389.2019.1634456.

Benalia, M.C., Youcef, L., Bouaziz, M.G., Achour, S., & Menasra, H. (2021). Removal of Heavy Metals from Industrial Wastewater by Chemical Precipitation: Mechanisms and Sludge Characterization. Arabian Journal for Science and Engineering. https://doi.org/10.1007/s13369-021-05525-7.

Bilgic, A. (2022). Fabrication of monoBODIPY-functionalized Fe_3O_4@SiO_2@TiO_2 nanoparticles for the photocatalytic degradation of rhodamine B under UV irradiation and the detection and removal of Cu(II) ions in aqueous solutions. Journal of Alloys and Compounds. 899, 163360. https://doi.org/10.1016/j.jallcom.2021.163360.

Chavan, V.D., Kothavale, V.P., Sahoo, S.C., Kollu, P., Dongale, T.D., Patil, P.S., & Patil, P.B. (2019). Adsorption and kinetic behavior of Cu(II) ions from aqueous solution on DMSA functionalized magnetic nanoparticles. Physica B: Condensed Matter. 571, 273–279. https://doi.org/10.1016/j.physb.2019.07.026.

Da, X., Li, R., Li, X., Lu, Y., Gu, F., & Liu, Y. (2022). Synthesis and characterization of PEG coated hollow Fe_3O_4 magnetic nanoparticles as a drug carrier. Materials Letters. 309, 131357. https://doi.org/10.1016/j.matlet.2021.131357.

Demirezen, D.A., Yılmaz, Ş., Yılmaz, D.D., & Yıldız, Y.Ş. (2022). Green synthesis of iron oxide nanoparticles using *Ceratonia siliqua L.* aqueous extract: Optimization, characterization, stabilization and evaluation of its antibacterial activity against gram-positive and gram-negative bacteria. http://dx.doi.org/10.2139/ssrn.4011560.

Dewi, S.H., & Adi, W.A. (2018). Synthesis and characterization of high purity Fe_3O_4 and α-Fe_2O_3 from local iron sand. Journal of Physics: Conference Series. 1091, 012021. https://doi.org/10.1088/1742-6596/1091/1/012021.

Dobaradaran, S., Nodehi, R.N., Yaghmaeian, K., Jaafari, J., Niari, M.H., Bharti, A.K., Agarwal, S., Gupta, V.K., Azari, A., & Shariatifar, N. (2018). Catalytic decomposition of 2-chlorophenol using an ultrasonic-assisted Fe_3O_4–TiO_2@MWCNT system: Influence factors, pathway and mechanism study. Journal of Colloid and Interface Science 512, 172–189. https://doi.org/10.1016/j.jcis.2017.10.015.

Eskandari, M.J., & Hasanzadeh, I. (2021). Size-controlled synthesis of Fe_3O_4 magnetic nanoparticles via an alternating magnetic field and ultrasonic-assisted chemical co-precipitation. Materials Science and Engineering B. 266, 115050. https://doi.org/10.1016/j.mseb.2021.115050.

Frei, E.H., Shtrikman, S., & Treves, D. (1957). Critical Size and Nucleation Field of Ideal Ferromagnetic Particles. Physical Review. 106, 446–455. https://doi.org/10.1103/PhysRev.106.446.

Guo, T., Bian, X., & Yang, C. (2015). A new method to prepare water based Fe_3O_4 ferrofluid with high stabilization. Physica A. 438, 560–567. http://dx.doi.org/10.1016/j.physa.2015.06.035.

Iorio, E.D., Colombo, C., Cheng, Z., Capitani, G., Mele, D., Ventruti, G., Angelico, R. (2019). Characterization of magnetite nanoparticles synthetized from Fe(II)/nitrate solutions for arsenic removal from water. Journal of Environmental Chemical Engineering. 7, 102986. https://doi.org/10.1016/j.jece.2019.102986.

Jabbar, K.Q., Barzinjy, A.A., & Hamad, S.M. (2022). Iron oxide nanoparticles: Preparation methods, functions, adsorption and coagulation/flocculation in wastewater treatment. Environmental Nanotechnology, Monitoring & Management. 17, 100661. https://doi.org/10.1016/j.enmm.2022.100661.

Janani, B., Al-Mohaimeed, A.M., Raju, L.L., Farraj, D.A.A. Thomas, A.M., & Khan, S. S. (2021). Synthesis and characterizations of hybrid PEG-Fe_3O_4 nanoparticles for the efficient adsorptive removal of dye and antibacterial, and antibiofilm applications. Journal of Environmental Health Science and Engineering. 19, 389–400. https://doi.org/10.1007/s40201-021-00612-1.

Jesus, A.C.B., Jesus, J.R., Lima, R.J.S., Moura, K.O., Almeida, J.M.A., Duque, J.G.S., & Meneses, C.T. (2020). Synthesis and magnetic interaction on concentrated Fe_3O_4 nanoparticles obtained by the co-precipitation and hydrothermal chemical methods. Ceramics International. 46, 11149–11153. https://doi.org/10.1016/j.ceramint.2020.01.135.

Jiao, Y., Wan, C., Bao, W., Gao, H., Liang, D., & Li, J. (2018). Facile hydrothermal synthesis of Fe_3O_4@cellulose aerogel nanocomposite and its application in Fenton-like degradation of Rhodamine B. Carbohydrate Polymers. 189, 371–378. https://doi.org/10.1016/j.carbpol.2018.02.028.

Karaagac, O., & Koçkar, H. (2022). Improvement of the saturation magnetization of PEG coated superparamagnetic iron oxide nanoparticles. Journal of Magnetism and Magnetic Materials. 551, 169140. https://doi.org/10.1016/j.jmmm.2022.169140.

Karimi, S., & Namazi, H. (2021). Fe_3O_4@PEG-coated dendrimer modified graphene oxide nanocomposite as a pH-sensitive drug carrier for targeted delivery of doxorubicin. Journal of Alloys and Compounds. 879, 160426. https://doi.org/10.1016/j.jallcom.2021.160426.

Kurniawan, A.V., Daud, A., & Sirajuddin, S. (2018). Risk Analysis Toxic Materials Borax and Rhodamine- B in Snack Against Primary School Children's Health in Housing Area of Tamalanrea Permai Makassar. ICHSM 18: Proceedings of the International Conference on Healthcare Service Management 2018. 30–34. https://doi.org/10.1145/3242789.3242795.

Leng, Y., Guo, W., Shi, X., Li, Y., & Xing, L. (2013). Polyhydroquinone coated Fe_3O_4 nanocatalyst for degradation of Rhodamine B based on sulfate radicals. Industrial & Engineering Chemistry Research. 52, 13607–13612. https://doi.org/10.1021/ie4015777.

Moosavi, S., Lai, C.W., Gan, S., Zamiri, G., Pivehzhani, O.A., & Johan, M.R. (2020). Application of Efficient Magnetic Particles and Activated Carbon for Dye Removal from Wastewater. ACS Omega. 5, 20684−20697. https://doi.org/10.1021/acsomega.0c01905.

Namikuchi, E.A., Gaspar, R.D.L., Silva, D.S., Raimundo, I.M., & Mazali, I.O. (2021). PEG size effect and its interaction with Fe_3O_4 nanoparticles synthesized by solvothermal method: morphology and effect of pH on the stability. Nano Express. 2, 020022. https://doi.org/10.1088/2632-959X/ac0596.

Ojemaye, M.O., & Okoh, A.I. (2019). Multiple nitrogen functionalized magnetic nanoparticles as an efficient adsorbent: synthesis, kinetics, isotherm and thermodynamic studies for the removal of rhodamine B from aqueous solution. Scientific Reports. 9, 9672. https://doi.org/10.1038/s41598-019-45293-x.

Peng, L., Qin, P., Lei, M., Zeng, Q., Song, H., Yang, J., Shao, J., Liao, B., & Gu, J. (2012). Modifying Fe_3O_4 nanoparticles with humic acid for removal of Rhodamine B in water. Journal of Hazardous Materials. 209–210, 193–198. https://doi.org/10.1016/j.jhazmat.2012.01.0.

Qian, L., Peng, J., Xiang, Z., Pan, Y., & Lu, W. (2019). Effect of annealing on magnetic properties of Fe/ Fe_3O_4 soft magnetic composites prepared by in-situ oxidation and hydrogen reduction methods. Journal of Alloys and Compounds. 778, 712e720. https://doi.org/10.1016/j.jallcom.2018.11.184.

Ramesh, A.V., Devi, D.R., Botsa, S.M., & Basavaiah, K. (2018). Facile green synthesis of Fe_3O_4 nanoparticles using aqueous leaf extract of Zanthoxylum armatum DC for efficient adsorption of methylene blue. Journal of Asian Ceramic Societies. 6(2), 145-155, https://doi.org/10.1080/21870764.2018.1459335.

Rangabhashiyam, S., Lins, P.V. S., Oliveira, Leonardo M.T.M., Sepulveda, P., Ighalo, J.O., Rajapaksha, A.U., & Meili, L. (2022). Sewage sludge-derived biochar for the adsorptive removal of wastewater pollutants: A critical review. Environmental Pollution. 293, 118581. https://doi.org/10.1016/j.envpol.2021.118581.

Ruiz, A., Alpízar, A., Beola, L., Rubio, C., Gavilán, H., Marciello, M., Ramiro, I.R., Ciordia, S., Morris, C.J., & Morales, M.P. (2019). Understanding the Influence of a Bifunctional Polyethylene Glycol Derivative in Protein Corona Formation around Iron Oxide Nanoparticles. Materials. 12, 2218. https://doi.org/doi:10.3390/ma12142218.

Salman, A.D., Juzsakova, T., Ákos, R., Ibrahim, R.I., Al-Mayyahi, M.A., Mohsen, S., Abdullah, T.A., & Domokos, E. (2021). Synthesis and surface modification of magnetic Fe_3O_4@SiO_2 core-shell nanoparticles and its application in uptake of scandium (III) ions from aqueous media. Environmental Science and Pollution Research. 28, 28428–28443. https://doi.org/10.1007/s11356-020-12170-4.

Seal, P., Alam, A., Borgohain, C., Paul, N., Babu, P.D., & Borah, J.P. (2021). Optimization of self heating properties of Fe_3O_4 using PEG and amine functionalized MWCNT. Journal of Alloys and Compounds. 882, 160653. https://doi.org/10.1016/j.jallcom.2021.160653.

Shen, Y.F., Tang, J., Nie, Z.H., Wang, Y.D., Ren, Y., & Zuo, L. (2009). Preparation and application of magnetic Fe_3O_4 nanoparticles for wastewater purification. Separation and Purification Technology. 68, 312–319. https://doi.org/0.1016/j.seppur.2009.05.020.

Shen, Y.F., Tang, J., Nie, Z.H., Wang, Y.D., Ren, Y., & Zuo, L. (2009). Tailoring size and structural distortion of Fe_3O_4 nanoparticles for the purification of contaminated water. Bioresource Technology. 100, 4139–4146. https://doi:10.1016/j.biortech.2009.04.004.

Sobeh, E.I., Amin, R., Saleh, H.M., Ali, S.E., & ElFeky, S.A. (2022). Evaluation of the radio-protective role of PEG-Fe_3O_4 NPs on γ-irradiated male Wistar rats. Environmental Nanotechnology, Monitoring & Management. 17, 100620. https://doi.org/10.1016/j.enmm.2021.100620.

Song, Y., Li, Y., Teng, Z., Huang, Y., Chen, X., & Wang, Q. (2018). Size-Controlled Synthesis of Carboxyl-Functionalized Magnetite Particles: Effects of Molecular Weight of the Polymer and Aging. ACS Omega. 3, 17904−17913. https://doi.org/10.1021/acsomega.8b02351.

Sultan, M.T., Al-Lami, H.S., & Al-Dujiali, A.H. (2019). Synthesis and characterization of alumina-grafted acrylic acid monomer and polymer and its adsorption of phenol and p-chlorophenol. Desalination and Water Treatment. 50, 192–203. https://doi.org/10.5004/dwt.2019.23593.

Suharyadi, E., Alfansuri, T., Handriani, L.S., Wibowo, N.A., & Sabarman, H. (2021). Detection of Fe_3O_4/PEG nanoparticles using one and two spin-valve GMR sensing elements in wheatstone bridge circuit. Journal of Materials Science: Materials in Electronics. 32, 23958–23967. https://doi.org/10.1007/s10854-021-06859-6.

Veisi, H., Moradi, S.B., Saljooqi, A., & Safarimehr, P. (2019). Silver nanoparticle-decorated on tannic acid-modified magnetite nanoparticles (Fe_3O_4@TA/Ag) for highly active catalytic reduction of 4-nitrophenol, Rhodamine B and Methylene blueMaterials Science & Engineering C. 100, 445–452. https://doi.org/10.1016/j.msec.2019.03.036.

Wang, Z., Wu, D., Wu, G., Yang, N., & Wu, A. (2013). Modifying Fe_3O_4 microspheres with rhodamine hydrazide for selective detection and removal of Hg^{2+} ion in water. Journal of Hazardous Materials. 244–245, 621–627. http://dx.doi.org/10.1016/j.jhazmat.2012.10.050.

World Health Organization. (2000). Obesity: preventing and managing the global epidemic (No. 894). World Health Organization.

Yongsheng, Y., He, L., Xu, J., Li, J., Jiang, S., Han, G., Jiang, B., Lei, W., Yang, W., & Hou, Y. (2022). A facile solution phase synthesis of directly ordering monodisperse FePt nanoparticles. Nano Research. 15, 446–451. https://doi.org/10.1007/s12274-021-3499-4.

Zhang, D., Cui, S., & Yang, J. (2017). Preparation of Ag_2O/g-C_3N_4/Fe_3O_4 composites and the application in the photocatalytic degradation of Rhodamine B under visible light. Journal of Alloys and Compounds. 708, 1141e1149. http://dx.doi.org/10.1016/j.jallcom.2017.03.095.

Zhang, H., Liu, X.L., Zhang, Y.F., Gao, F., Li, G.L., He, Y., Peng, M.L., & Fan, H.M. (2018). Magnetic nanoparticles based cancer therapy: current status and applications. Science China Life sciences. 61. https://doi.org/10.1007/s11427-017-9271-1.

Zhang, Y., Su, P., Weathersby, D., Zhang, Q., Zheng, J., Fan, R., Zhang, J., & Dai, Q. (2020). Synthesis of γ-Fe_2O_3-ZnO-biochar nanocomposites for Rhodamine B removal. Applied Surface Science. 501, 144217. https://doi.org/10.1016/j.apsusc.2019.144217.

Zhu, H. Y., Fu, Y.Q., Jiang, R., Jiang, J.H., Xiao, L., Zeng, G.M., Zhao, S.L., & Wang, Y. (2011). Adsorption removal of congo red onto magnetic cellulose/Fe_3O_4/activated carbon composite: Equilibrium, kinetic and thermodynamic studies. Chemical Engineering Journal. 173, 494–502. https://doi.org/10.1016/j.cej.2011.08.020.